

# Generalized Concatenation of Encoded Gaussian Filtered Continuous Phase Modulation<sup>\*†</sup>

Martin Bossert, Günther Haas

Dept. of Information Technology  
University of Ulm, Germany  
{boss,haas}@it.e-technik.uni-ulm.de

Sergo Shavgulidze

Georgian Technical University  
Tbilisi, Georgia  
sergo\_130@hotmail.com

Armin Häutle, Hans Dieterich

Siemens AG, ICN CA MR EK5  
Ulm, Germany  
Armin.Haeutle@icn.siemens.de

*Abstract*— In this paper, we introduce the construction of generalized concatenated (multilevel) encoded Gaussian filtered CPM systems. It is shown that the constructed multilevel codes may operate with coherent and noncoherent demodulation of signals and can be used in Gaussian and Rayleigh-fading channels. The simulation results are presented for both channel types. We show that the proposed systems have error performance advantages over the known constructions taken from the literature.

## I. INTRODUCTION

CONTINUOUS phase modulation (CPM) is known as a power and spectral efficient modulation scheme suitable for application in digital communication systems [1]. An important property of CPM is its constant envelope, which avoids the necessity of expensive linear amplifiers.

In this work, we consider  $M$ -ary Gaussian filtered CPM (GCPM). This includes the frequently used binary case known as Gaussian minimum shift keying (GMSK) [2]. For GMSK, the alphabet size is  $M = 2$  and the modulation index is  $h = 1/2$ . The traditional approach is to construct encoded GMSK systems by matching binary convolutional codes, and joint demodulation and decoding in the combined supertrellis by means of maximum-likelihood sequence detection based on the Viterbi algorithm [3]. In [4] an alternative two-stage receiver was also investigated consisting of separate demodulation of GMSK followed by decoding of the convolutional code. We refer to this procedure as concatenated decoding (CD).

It was shown in [5] how generalized concatenated codes (GCC) (or multilevel codes) can be constructed on the basis of inner modulation with memory, namely tamed frequency modulation. Here an additive white Gaussian noise (AWGN) channel and coherent demodulation was assumed. In this paper, we apply this approach to GCPM signals which can be used for noncoherent demodulation as well. In addition, we show some simulated bit error rate performance results for the Rayleigh-fading channel.

<sup>\*</sup>This work was in part supported by the *Deutsche Forschungsgemeinschaft DFG* in Bonn, Germany.

<sup>†</sup>Revised Version (V2)

## II. SYSTEM DESCRIPTION

### A. Modulation

In general, for CPM the transmitted signal can be described by [1]

$$s(t, \underline{v}) = \sqrt{\frac{2E}{T}} \cos(2\pi f_c t + \Phi(t, \underline{v}) + \Phi_0)$$

where  $E$  is the symbol energy,  $f_c$  is the carrier frequency,  $T$  is the symbol time and  $\Phi_0$  is a constant arbitrary phase offset. The information-carrying phase is given by  $\Phi(t, \underline{v}) = 4\pi h \sum_{n=0}^{\infty} v_n q(t - nT)$  where  $\underline{v} = v_0, v_1, \dots, v_n, \dots$  is a semi-infinite sequence of  $M$ -ary symbols  $v_n \in \{0, 1, \dots, M-1\}$  and  $h$  is the modulation index. The phase response is defined by  $q(t) = \int_{-\infty}^t f(\tau) d\tau$  where  $f(t)$  is the frequency response.

For Gaussian filtered CPM, the frequency response can be expressed as

$$f(t) = \frac{1}{2T} \left[ Q \left( 2\pi B \frac{t - T/2}{\sqrt{\ln 2}} \right) - Q \left( 2\pi B \frac{t + T/2}{\sqrt{\ln 2}} \right) \right]$$

where  $Q(t) = \int_t^{\infty} (1/\sqrt{2\pi}) \exp(-\tau^2/2) d\tau$  and  $BT$  is the normalized bandwidth. Since the frequency pulse has an infinite duration, it is limited for practical reasons to  $L$  symbol intervals such that  $q(LT) = 1/2$  is satisfied. The pulse length  $L$  can be considered as the memory of the modulator and its value should be chosen large enough to preserve the spectral characteristics.

If we view GCPM as an  $L$ -response GCPM scheme, it allows one to apply the “tilted” representation of CPM signals as introduced in [6]. Using this description, the GCPM modulator can be decomposed into a time-invariant memoryless modulator and a time-invariant continuous phase encoder with memory which we call the GCPM encoder. For simplicity, we will focus on  $M$ -ary modulation with input  $v_n \in \{0, 1, \dots, M-1\}$  and modulation index  $1/M$ . Then the GCPM modulator can be described by Fig. 1.

It follows from Fig. 1 that the modulator state can be uniquely described by the  $L$ -tuple

$$(v_{n-1}, v_{n-2}, \dots, v_{n-L+1}, c_n)$$

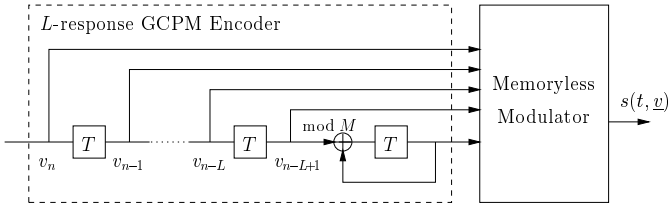


Fig. 1. Decomposition model of the  $L$ -response GCPM modulator.

where  $c_n = \sum_{i=0}^{n-L} v_i \pmod{M}$ . Therefore,  $M$ -ary GCPM with  $h = 1/M$  can be represented by means of a trellis diagram which contains  $M^L$  nodes (states) on each tier and each node consists of  $M$  incoming and  $M$  outgoing branches.

It can be seen from Fig. 1 that the conventional GCPM encoder model results in an encoder with feedback. If the  $M$ -ary input symbols of the GCPM modulator are differentially encoded by a conventional precoder with transfer function  $T(D) = 1 - D$  (subtraction is carried out modulo  $M$ ), an equivalent feedback-free GCPM modulator with the same number of states is obtained. For details see [6].

### B. Partitioning Principle

For the construction of GCC, a partitioning method is needed which partitions the inner system (code or modulation) into nested subsystems with improved characteristics, e.g. Euclidean distance. In order to construct GCC based on inner modulation with memory, i.e. GCPM, we apply the partitioning using a scrambler as presented in [5] and [?].

Consider the trellis diagram of GCPM where each path in the trellis corresponds to a transmitted GCPM signal. In order to obtain a subsystem of GCPM signals, a path puncturing method can be considered where paths are periodically deleted. The reduced set of trellis paths gives the subsystem. The idea is to puncture the paths having a small free Euclidean distance. Unfortunately, using the input sequence directly for puncturing does not always improve the partitioning in terms of distances. A scrambler is used to change the information to code sequence mapping which allows to carry out the efficient path puncturing procedure. Therefore, the cascade of a scrambler and the original GCPM encoder is considered that results in an equivalent GCPM encoder.

A systematic computer search was performed to find for GCPM the best scrambler matrices  $C_m$  for  $m = 2, 3, 4$  partitioning levels. The results are listed in Tables I and II where  $\delta^{2,(j)}$  is the normalized (by  $2E_b$  and  $E_b$  denotes the energy per bit) squared free Euclidean distance in the GCPM (sub)system step  $j$ ,  $j = 1, 2, \dots, m$ .

We used the sign “ $m$ ” in order to differentiate between two possible scrambler matrices with the same number of partitioning levels.

### C. Generalized Concatenated GCPM Scheme

Now we are able to construct a generalized concatenated code using the partitioning of the inner code (GCPM).

TABLE I  
SCRAMBLER MATRICES FOR GMSK

$C_m$	Scrambler	$j$	$\delta^{2,(j)}$	
			$BT = 0.25$	$BT = 0.3$
$C_2$	$\begin{pmatrix} 1 & 0 \\ 1+D & 1 \end{pmatrix}$	1	1.75	1.82
		2	6.00	6.00
$C_2'$	$\frac{1}{1+D} \begin{pmatrix} 1 & 1 \\ D & 1 \end{pmatrix}$	1	1.75	1.82
		2	4.00	4.00
$C_3$	$\begin{pmatrix} 0 & 1 & 0 \\ 1 & 1 & 0 \\ D & 1+D & 1 \end{pmatrix}$	1	1.75	1.82
		2	3.19	3.42
		3	8.00	8.00
$C_4$	$\begin{pmatrix} 1 & 1 & 0 & 0 \\ 0 & 1 & 1 & 0 \\ 1 & 1 & 1 & 0 \\ 1 & 1+D & D & 1 \end{pmatrix}$	1	1.75	1.82
		2	1.75	1.82
		3	6.00	6.00
		4	9.13	9.39

TABLE II  
SCRAMBLER MATRICES FOR QUATERNARY GCPM ( $BT = 0.3$ ) WITH  
 $h = 1/4$

$C_m$	Scrambler	$j$	$\delta^{2,(j)}$
$C_2$	$\begin{pmatrix} 1 & D \\ D & 1+D^2 \end{pmatrix}$	1	1.09
		2	5.11
$C_4$	$\begin{pmatrix} D^2 & 1+D & 1+D & 1+D^2 \\ 1+D & 1 & 1 & 1+D \\ D+D^2 & D & D & 1+D+D^2 \\ D+D^2 & 1+D & D & 1+D+D^2 \end{pmatrix}$	1	1.09
		2	1.20
		3	3.63
		4	9.68

Since each of the  $m$  subsystems of signals may have different distance characteristics, we can use  $m$  outer convolutional codes with error-correcting capabilities adapted to the corresponding inner subsystems. Below we briefly describe the procedures of encoding and decoding which are similar to the TFM case [5].

The binary information sequence is divided into  $m$  subsequences which are separately encoded by  $m$  independent convolutional encoders. Then the outputs of all encoders are either first interleaved or used directly as the scrambler input sequences. The  $m$  binary output sequences of the scrambler are serialized (then mapped onto an  $M$ -ary sequence, if  $M > 2$ ), and the resulting sequence is fed into the precoded GCPM modulator. As a result of encoding and modulation, we obtain the sequence of a generalized concatenated code with inner nested GCPM signals and outer convolutional codes. As the  $j$ th outer convolutional code,  $j = 1, 2, \dots, m$ , we use binary codes with parameters  $(n_j, k_j, d_f^{(j)})$  and constraint length  $\nu_j$  where  $d_f^{(j)}$  denotes the free Hamming distance. The overall code rate of GCC  $R = (1/m) \sum_{j=1}^m R_j$ , with  $R_j = k_j/n_j$ .

The generalized concatenated decoding (GCD) algorithm of GCC consists of  $m$  steps. Each step contains inner-stage demodulation of signals and outer-stage decoding of the convolutional codes. In the first step, the received signal is demodulated on the basis of the original GCPM trellis diagram. This procedure can be carried out by the symbol by symbol maximum *a posteriori* probability (MAP) algorithm [7] or the less complex soft-output Viterbi algorithm (SOVA) [8], which can be easily applied to CPM trellis diagrams. This results in soft-output, which is used as soft-input information for the decoder of the first

outer convolutional code. Then, the first outer convolutional code is decoded by means of Viterbi algorithm [3]. As a result of the decoding, we obtain the information sequence which was encoded by the first outer encoder. The decoded (and deinterleaved) sequence uniquely defines the subtrellis that can be used in the second step of the algorithm. Consequently, we can demodulate the received signal again, but now according to the nested subtrellis. The result of this demodulation is used as input for the second outer convolutional code and so on. In general, the received signal is demodulated at the  $j$ th step based on the  $j$ th nested GCPM subtrellis. Based on this decoding result, the subtrellis is constructed for the  $(j + 1)$ th step.

The GCD algorithm can be applied both with coherent and noncoherent demodulation at the inner stage. First let us focus our attention on GMSK signals and transmission over an AWGN channel. So far only coherent demodulation of GMSK signals has been considered. In the following, we investigate the noncoherent case. Assume the signal  $s(t, \underline{v})$  is transmitted, and the signal

$$r(t) = s(t, \underline{v}) + n(t)$$

is received where  $n(t)$  is the noise.

In [9], the Viterbi algorithm was used for noncoherent demodulation of CPM signals which includes GMSK. However, this approach is limited to hard-output decisions. For performance reasons, the soft output Viterbi algorithm (SOVA), originally introduced by Hagenauer and Hoehner [8], was proposed for noncoherent demodulation of GMSK signals [10]. In [11], a simplified receiver is described for differential binary phase shift keying which allows differential detection. In the following we apply the same rule to GMSK using the scrambler  $C'_2$  given in Table I which allows differential detection for coherent and noncoherent demodulation. The resulting modulator can be considered as the cascade of a recursive scrambler, described by the matrix

$$\frac{1}{1+D} \begin{pmatrix} 1 & 1 \\ D & 1 \end{pmatrix},$$

and a precoded (non-recursive) GMSK encoder with transfer function

$$(D, D^2, \dots, D^L).$$

Since we use a simplified receiver for GMSK which allows differential detection, we inherently assume  $L = 1$  at the receiver stage. Hence, the inner scrambled and precoded GMSK encoder can be described by the matrix<sup>1</sup>

$$\frac{1}{1+D} \begin{pmatrix} D & 1 \\ D & D \end{pmatrix}.$$

Thus, the inner modulation results simply in a non-precoding GMSK modulator.

<sup>1</sup>Corrected after publication in *Conference Record 3rd ITG Conference, Source and Channel Coding*, ITG Fachbericht 159, pages 133–137, Munich, Germany, January 2000. There accidentally the wrong matrix  $\frac{D}{1+D} \begin{pmatrix} 1 & 1 \\ D & 1 \end{pmatrix}$  was given.

Now consider the encoding and decoding schemes for this particular case (Fig. 2). We denote  $\underline{y}^{(1)}$  and  $\underline{y}^{(2)}$  as the binary information sequences and  $\underline{z}^{(1)}$  and  $\underline{z}^{(2)}$  as the encoded sequences for the first and second outer encoders, respectively. The encoded sequences are serialized and directly used as the input sequence  $\underline{v}$  of the GMSK modulator.

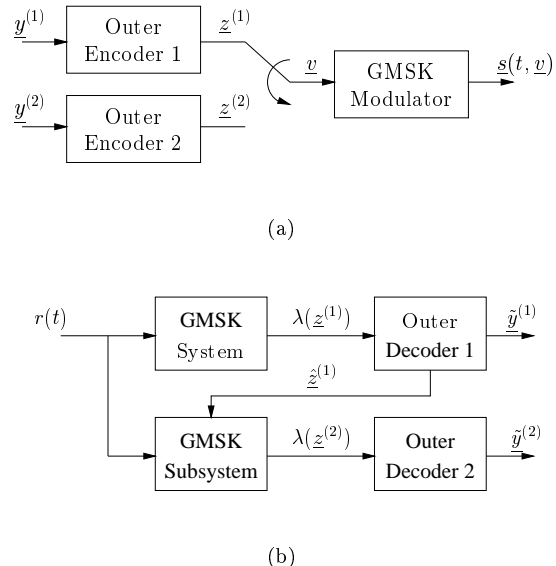


Fig. 2. Generalized concatenated encoder (a) and decoder (b) for  $m = 2$ .

In the first demodulation step, i.e.  $j = 1$ , we derive the soft-output information for the encoded binary sequence  $\underline{z}^{(1)} = (z_0^{(1)}, z_1^{(1)}, \dots, z_n^{(1)}, \dots)$  of the first outer code from

$$\lambda(z_n^{(1)}) = \text{Re}(y_{2n-1} y_{2n-2}^*) \quad (1)$$

where  $y_n$  denotes the derotated sample at time  $t = nT$  obtained from the received sample  $r_n$  by  $y_n = r_n \exp(j\pi/2)$ , and “\*” is the complex conjugate operator. The soft output sequence  $\lambda(\underline{z}^{(1)})$  is delivered to the first outer decoder. As a result of decoding, we get the first information sequence  $\hat{\underline{y}}^{(1)}$  and its corresponding code sequence  $\hat{\underline{z}}^{(1)} = (\hat{z}_0^{(1)}, \hat{z}_1^{(1)}, \dots, \hat{z}_n^{(1)}, \dots)$ . For notation purposes, we set  $\hat{z}_n^{(1)} = 0 \rightarrow +1$  and  $\hat{z}_n^{(1)} = 1 \rightarrow -1$ .

In the second demodulation step, we use the sequence  $\hat{\underline{z}}^{(1)}$  and derive the soft-output information for the encoded binary sequence  $\underline{z}^{(2)} = (z_0^{(2)}, z_1^{(2)}, \dots, z_n^{(2)}, \dots)$  of the second outer code from

$$\lambda(z_n^{(2)}) = \text{Re}(y'_{2n} y'_{2n-1}^*) \quad (2)$$

Here  $y'_{2n} = (y_{2n} + \hat{z}_{n+1}^{(1)} y_{2n+1})/2$  and  $y'_{2n-1} = (y_{2n-1} + \hat{z}_n^{(1)} y_{2n-2})/2$  are normalized variables taking into account the results of the first outer decoding.

This soft-output information is used as a soft-input for the second outer Viterbi decoder that yields the second information sequence  $\hat{\underline{y}}^{(2)}$ .

### III. SIMULATION RESULTS

In this section, we present the simulated bit error rates (BER) of concatenated and generalized concatenated GCPM based on known binary convolutional codes. We chose a block interleaver with depth of 10 rows which was sufficient to avoid the dependence of errors in the consecutive symbols of each outer code.

First, consider transmission over an AWGN channel and coherent demodulation of GCPM signals. In order to preserve the spectral characteristics, we consider the GCPM transmitter as a 4-response CPM scheme. However, for complexity reasons, the GCPM (sub)systems are demodulated on the basis of  $M^2$ -state trellis diagrams, i.e. the case when  $L = 2$ . In the following constructions, we used outer binary convolutional codes which have the same state complexity  $W$  as the modulation system, i.e.  $W = 4$  states for GMSK and  $W = 16$  states for quaternary GCPM. The code parameters were taken from [12] and [13].

In Fig. 3, we show the simulation results of rate  $R = 2/3$  and  $R = 1/2$  encoded GMSK based on the scrambler matrices  $C_2$  and  $C_3$  which are given in Table I. We have chosen the outer code parameters  $(n_j, k_j, d_f^{(j)})$  as follows. For  $R = 2/3$  —  $C_2$ : first code (3,1,8), second step uncoded;  $C_3$ : first code (3,2,3), third step uncoded. For  $R = 1/2$  —  $C_2$ : first code (5,1,13), second punctured code (5,4,2);  $C_3$ : first code (6,1,16), second punctured code (9,4,6), third punctured code (9,8,2). All convolutional codes have the same constraint length  $\nu = 2$ .

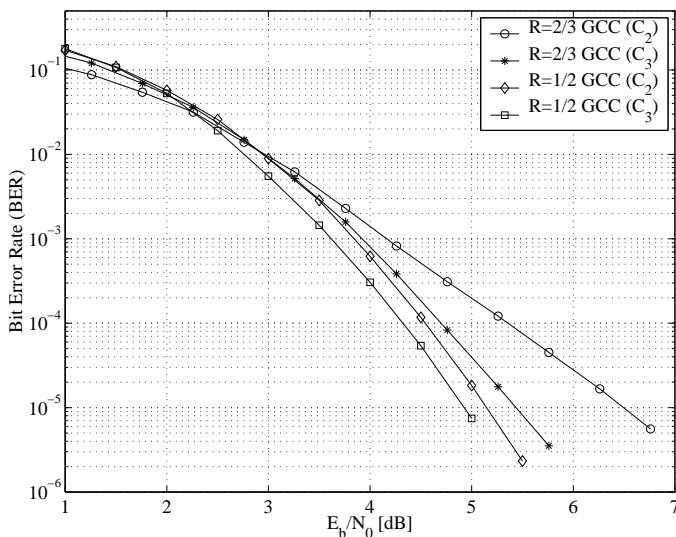


Fig. 3. Rate  $R = 1/2$  and  $R = 2/3$  encoded GMSK with  $BT = 0.3$ ; coherent demodulation;  $W = 4$ .

In Fig. 4, we show the BER performance of rate  $R = 2/3$  and  $1/2$  encoded quaternary GCPM based on the scrambler matrix named  $C_2$  in Table II, and uncoded GMSK and quaternary GCPM. The rate- $2/3$  GCC is constructed based on a single (3, 1, 12) convolutional code. The second step remains uncoded. The rate- $1/2$  GCC is constructed based on first code (14, 1, 56) and second punctured code (14, 13, 2).

All convolutional codes have the same constraint length  $\nu = 4$ . It can be seen from Fig. 4 that having the same transmission rate (1 bit per symbol) the rate- $1/2$  encoded GCPM scheme achieves a gain of approximately 4 dB at a BER of  $10^{-5}$  compared to uncoded GMSK.

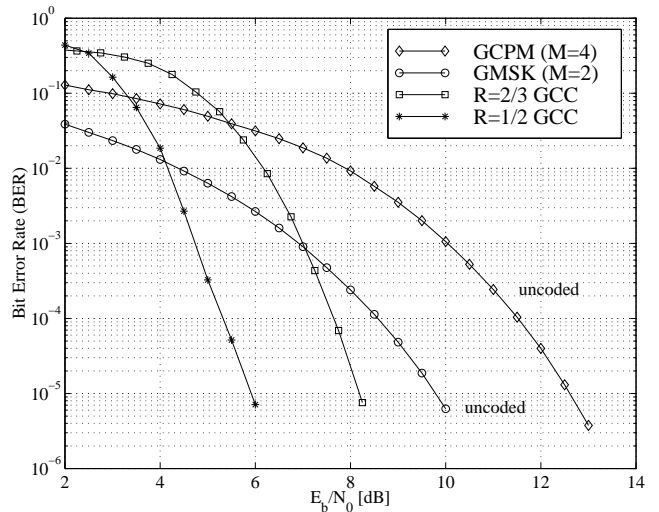


Fig. 4. Rate  $R = 1/2$  and  $R = 2/3$  encoded GCPM with  $BT = 0.3$ ; coherent demodulation;  $W = 16$ .

The AWGN channel is the channel model most commonly assumed for the performance evaluation of encoded modulation schemes. However, for many systems, such as mobile radio or satellite communication, data is transmitted over a fading channel. In general, optimal codes for the AWGN channel are not always the optimal for fading channels, and vice versa. However, the characteristics of some channels may vary between the features of an AWGN channel and those of a fading channel. It is therefore advantageous to design codes which perform well in both environments. We note that our GCC constructions can be used both on Gaussian and fully interleaved frequency non-selective slowly fading channels. In such a model the fading amplitude is assumed to be Rician distributed and constant for one symbol interval. The Rice factor  $\xi$  denotes the ratio of the signal energy of a dominant path to the energy of the diffuse paths. For  $\xi = 0$  we have Rayleigh fading, and for  $\xi \rightarrow \infty$  the fading channel reduces to the nonfading Gaussian channel.

In order to compare two approaches, the one given in [4] and the second described here, we present in Fig. 5 simulation results in the AWGN and fully interleaved Rayleigh-fading channel for concatenated code (CC) and GCC ( $m = 2$ ) based on inner GMSK and outer binary convolutional codes. Our model assumed CD and GCD algorithm respectively with inner noncoherent demodulation. For CC construction, we used the convolutional code (2, 1, 5). For GCC we have chosen the code (4, 1, 10) as the first code, and the punctured code (4, 3, 3) as the second code. Thus, as in the CC case, the GCC has overall code rate  $1/2$ . Furthermore, all convolutional codes have the same constraint length  $\nu = 2$ .

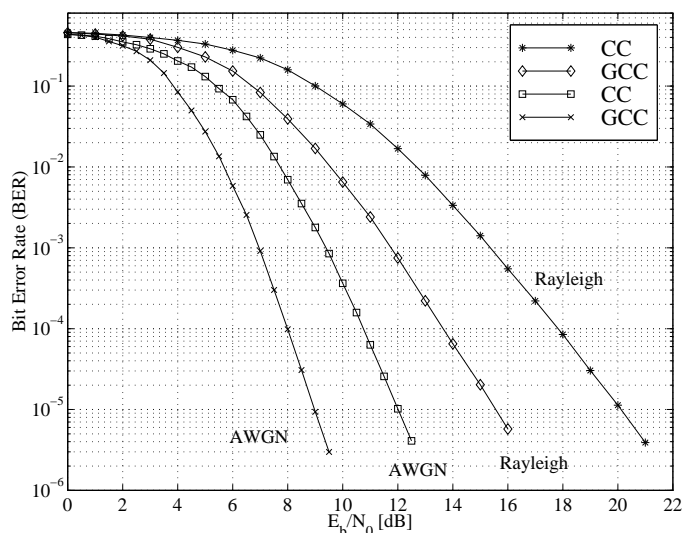


Fig. 5. Rate  $R = 1/2$  encoded GMSK with  $BT = 0.25$ ; noncoherent demodulation;  $W = 4$ .

The overall receiver complexity including demodulation and decoding for CC and GCC is mainly determined by the decoding of the outer code(s). In the case of CC, we assume Viterbi decoding of a single rate- $1/2$  outer code on the basis of a 4-state trellis. The branch complexity per decoded information bit of this code is equal to  $4 \cdot 2 = 8$ . For GCC, we used a rate- $1/4$  and a punctured rate- $3/4$  code, both with 4-state complexity. As a result, we obtain a branch complexity of  $(2 \cdot 4 + 3 \cdot 2 \cdot 4) / 4 = 8$  per information bit which is the same as in the CC case. However, the GCC shows a significant coding gain in comparison with the CC.

#### REFERENCES

- [1] J. B. Anderson, T. Aulin, and C.-E. Sundberg, *Digital Phase Modulation*. New York: Plenum, 1986.
- [2] K. Murota and K. Hirade, "GMSK modulation for digital mobile radio telephony," *IEEE Trans. Commun.*, vol. COM-29, pp. 1044-1050, July 1981.
- [3] G. D. Forney, Jr., "The Viterbi algorithm," *IEEE Proc.*, vol. 61, pp. 268-278, Mar. 1973.
- [4] P. Tyczka and W. Holubowicz, "Comparison of several receiver structures for trellis-coded GMSK signals: Analytical and simulation results," in *IEEE Int. Symp. on Inform. Theory*, (Ulm, Germany), p. 193, June/July 1997.
- [5] M. Bossert, S. Shavgulidze, A. Häutle, H. Dieterich, "Generalized concatenation of encoded tamed frequency modulation," *IEEE Trans. Commun.*, vol. COM-42, pp. 1337-1345, Oct. 1998.
- [6] B. Rimoldi, "A decomposition approach to CPM," *IEEE Trans. Inform. Theory*, vol. IT-34, pp. 260-270, Mar. 1988.
- [7] L. R. Bahl, J. Cocke, F. Jelinek, and J. Raviv, "Optimal decoding of linear codes for minimizing symbol error rate," *IEEE Trans. Inform. Theory*, vol. IT-20, pp. 284-287, Mar. 1974.
- [8] J. Hagenauer and P. Hoeher, "A Viterbi algorithm with soft-decision outputs and its applications," *Proc. IEEE GLOBECOM '89*, vol. 3, pp. 1680-1686, Nov. 1989.
- [9] G. Colavolpe and R. Raheli, "Noncoherent sequence detection of CPM," *Electron. Lett.*, vol. 34, pp. 259-261, Feb. 1998.
- [10] H. Mathis, "Differential detection of GMSK signals with low  $B_tT$  using the SOVA," *IEEE Trans. Commun.*, vol. COM-46, pp. 428-430, Apr. 1998.
- [11] J. G. Proakis, *Digital Communications*. New York: McGraw-Hill, 1989.
- [12] R. Palazzo Jr., "A network flow approach to convolutional codes," *IEEE Trans. Commun.*, vol. COM-43, pp. 1429-1440, Feb./Mar./April 1995.

- [13] Y. Yasuda, K. Kashiki, and Y. Hirata, "High-rate punctured convolutional codes for soft decision Viterbi decoding," *IEEE Trans. Commun.*, vol. COM-32, pp. 315-319, Mar. 1984.